ARTICLE OPEN

Check for updates

ADHD symptoms across the population are explained by individual variability in brain criticality

Hamed Haque[1,2,3,9], Jonni Hirvonen[1,9], Sheng H. Wang[1,4,5], Jaana Simola[1,6], Isabel Morales-Muñoz[1,7], Benjamin U. Cowley[6,8], J. Matias Palva[1,3,4] and Satu Palva[1,3]✉

© The Author(s) 2026

Attention-deficit/hyperactivity disorder (ADHD) is characterized by a continuum of symptoms, including inattentiveness, impulsiveness, and hyperactivity, which can negatively impact daily life. In laboratory settings, these deficits are manifested as increased reaction-time variability in continuous performance tasks (CPTs) over several minutes. Although considerable work has elucidated neural mechanisms associated with ADHD, less is known about how these mechanisms vary across the continuum of symptom severity. We investigated whether symptom severity could be explained in the Extended Brain Criticality framework. Brains operate in an extended critical regime between disorder (asynchronous) and order (synchronous) at balanced excitation-inhibition which is characterized by moderate synchronization and scale-free long-range temporal correlations (LRTCs) across hundreds of seconds. We hypothesized that differences in brain operating points (brain states) along the critical-like regime and paralleled changes in LRTCs could predict ADHD symptom continuum. We measured brain activity with magnetoencephalography (MEG) during rest and two CPTs from adult ADHD and control participants and assessed criticality with LRTCs of neuronal oscillations. LRTCs showed high variability, but overall ADHD patients exhibited stronger LRTCs than NC in low (5-20 Hz) and high (30-100 Hz) frequencies as well as stronger task effects. ADHD symptom severity was predicted by individual variability in LRTCs and i.e., by the individual's position in the critical phase with both linear and quadratic correlations such that the severity of symptoms were predicted by shifts of the operating point toward the supercritical direction in a frequency dependent manner. Our study thus proposes a novel complex systems-level framework to explain the emergence of ADHD symptoms and their continuum across the population.

Translational Psychiatry (2026)16:645 ; https://doi.org/10.1038/s41398-026-04267-0

INTRODUCTION

Attention-deficit/hyperactivity disorder (ADHD) is a heritable neurodevelopmental condition characterized by detrimental levels of impulsive, inattentive and/or hyperactive traits [1], which have adverse influence on many domains of daily life. In adults, symptoms include insufficient inhibitory control, defects in working memory, impaired socioemotional processing, and challenges in completing tasks that require sustained self-regulation of attention [2]. As of relevance, ADHD is often comorbid with anxiety and mood disorders underscoring the heterogeneity in symptom profiles, which suggest diverse underlying transdiagnostic neural mechanisms of symptoms [3, 4]. In laboratory settings, continuous performance tasks (CPTs) with elementary decisions (yes/no) are often used to study fluctuations in performance and decision-making along with tasks measuring attentional allocation, response inhibition and executive functions. One of the markers of cognitive dysfunction in individuals with ADHD is increased reaction time variability (RTV) [5–7], which is thought to reflect intermittent drifts in attention, attentional impulsiveness and deficits in executive function [8, 9]. One influential approach to understanding this variability has been the sequential sampling models (SSMs), which model how individuals accumulate information until a threshold of evidence [10]. These have provided converging evidence that ADHD is associated with reduced drift rates, i.e. the integration of information [11–13]. Despite ADHD being often considered as a negative disorder, individuals with ADHD have often been shown to exhibit hyper-focus on highly motivating tasks [14, 15], and adaptive features such as novelty-seeking [16] that can be beneficial features in changing environments.

At the neural level, in functional MRI (fMRI) both increased and decreased functional connectivity (FC) have been found among default mode network (DMN), fronto-parietal network (FPN), and salience networks [17–20], with FC alterations serving as a robust biomarker for ADHD [21]. In electrophysiological recordings with electro- and magnetoencephalography (EEG/MEG) that yield direct millisecond temporal precision view on neural activity, a decade of investigations in the time domain have established that

[1]Neuroscience Center, Helsinki Institute of Life Science, University of Helsinki, Helsinki, Finland. [2]BioMag laboratory, HUS Medical Imaging Center, Helsinki, Finland. [3]School of Psychology and Neuroscience, University of Glasgow, Glasgow, UK. [4]Department of Neuroscience and Biomedical Engineering, Aalto University, Espoo, Finland. [5]Jack H. Miller MEG Center, Helen DeVos Children's Hospital, Corewell Health, Grand Rapids, Michigan, USA. [6]Faculty of Educational Sciences, University of Helsinki, Helsinki, Finland. [7]Institute for Mental Health, School of Psychology, University of Birmingham, Birmingham, UK. [8]Cognitive Science, Department of Digital Humanities, Faculty of Arts, University of Helsinki, Helsinki, Finland. [9]These authors contributed equally: Hamed Haque, Jonni Hirvonen. ✉email: satu.palva@helsinki.fi

Received: 4 March 2025 Revised: 4 June 2026 Accepted: 6 July 2026
Published online: 20 July 2026

event related potentials (ERPs) are associated with early orienting, inhibitory control, and error-processing differ in ADHD [22–25]. These changes include reduced P3 amplitude [26–29] thought to reflect decreased attentional allocation and reduced P2 reflecting thought to reflect early inhibition processes [30]. More recently, time-frequency approaches have also found evidence for spectral differences in ADHD. Alpha (α, 8 − 13 Hz) and beta (β, 20 − 30 Hz) band oscillations, which are fundamental for coordinating attention and top-down control [31–34], show reduced task-dependent suppression and lateralization of local oscillation amplitudes in adults [25, 26, 35–37], adolescents [35, 38, 39], and children [40–42] with ADHD. In addition, mid-frontal theta-band oscillations show differences in ADHD putatively associated with executive function deficits [43–46]. Taken together, dynamic and transient modulations of ERPs and brain oscillations are thought to reflect mechanisms underlying task performance differences in ADHD.

However, the neural mechanisms underlying variability across long-time scales have remained less understood. The brain criticality framework offers a statistical-physics mechanism for understanding this variability, positing that brains operate in a critical regime near a critical transition point between subcritical (disorder) and supercritical (order) phases, respectively [47–53]. Importantly, such operation at the critical regime (phase) yields scale-free 1/f long-range temporal correlations (LRTCs) of neuronal activity and oscillations, associated with functional benefits, such as maximal dynamic range, information transmission, and representational capacity, which support optimal brain function [52, 54, 55]. The primary control parameter responsible for tuning the operating-point is the net functional excitation/inhibition (E/I) ratio whereby criticality is a key endpoint of neuronal homeostatic control [56] such that a perfectly balanced E/I leads to operation at the critical point [57, 58]. While excessive inhibition or excitation leads to operation in the sub- or supercritical phases [59, 60]. In the critical point, the incoming activity is neither amplified (supercritical) nor damped (subcritical) but approximately preserved as it passes through neural networks. Healthy individuals operate at a slightly subcritical side to the critical point, but nevertheless great variability is expressed in the individual operating points across individuals, brain areas and frequencies [61, 62]. This is in line with the recent theoretical framework in which structural and biological heterogeneity leads to a more realistic brain dynamics and to extended critical regime [63–66] or quasicriticality [67]. Further, in computational models, optimal performance is associated with dynamic movement within the critical regime [63, 68] also supported by some behavioral [69] and neural data [70, 71]. In contrast, many brain disorders are associated with E/I imbalance [72–74], epileptiform hyper-synchronized activity [61, 75] and associated with shifts toward super-critical excitation-driven dynamics pathophysiological dynamics [74].

The net E/I balance is modulated by multi-dimensional factors across cortical sites and dynamically across timescales such as different subtypes of GABAergic inhibitory interneurons involving complex feedback mechanism [76], the ascending arousal system (AAS) of noradrenergic and cholinergic neuromodulations [77], and other neurotransmitter systems. Importantly, ADHD is associated with a shift in net E/I towards greater excitability through both elevated glutamatergic excitation and GABAergic inhibitory deficits [78, 79] as well as in norepinephrine (NE) and dopamine (DA) levels [80, 81]. Conversely, the primary stimulant and non-stimulant medications for ADHD act on the NE and dopamine pathways to increase their availability in AAS projection targets [82–84]. We thus hypothesized that elevated cognitive variability in ADHD could be caused by impairments in net E/I balance, thereby shifting the operating point towards more excitation-dominated brain dynamics.

Oscillations exhibit long-range temporal correlations (LRTCs) in their amplitude envelopes lasting from seconds to minutes. As LRTCs peak at the idealized critical point, they are considered as a proxy for critical brain dynamics [48, 85] albeit LRTCs can also exist without criticality [86]. As of importance, LRTCs are associated with subsecond time-scale oscillation FC in experimental data [61] and computational models [87] and are therefore linked to previous findings of aberrancies of fast oscillation aberrancies. Furthermore, the inter-individual variability in neuronal LRTCs is linked with LRTCs in behavioral performance in CPT tasks, and, consequently, with the lengths of behavioral streaks [88–90] thus linking criticality with behavioral fluctuations. Finally, LRTCs are dependent on the variability of neuromodulatory [91] genes. Previous studies show attenuated LRTCs in Alzheimer's disease [74, 92], schizoaffective disorders [93, 94], and major depressive disorder [95, 96], and increased LRTCs in epilepsy [97], and mixed findings for autism spectrum disorder [73, 98, 99].

Despite ADHD being associated with increased RTV, shifts in attentional states, and impulsivity in CPTs — indicating aberrant behavioral fluctuations on timescales greater than 100 s — there is no direct evidence linking ADHD symptoms to altered LRTCs in neuronal dynamics. A single prior study has addressed whether ADHD was associated with altered LRTCs but found no evidence to this effect [100].

We thus tested here the hypothesis that ADHD symptoms could be explained in the brain criticality framework by shifts in individual operating points toward the supercritical side of the extended critical regime (Fig. 1). To test this, we recorded MEG data during two different CPTs from adult ADHD and neurotypical control (NC) participants and estimated LRTCs from MEG oscillation amplitude fluctuations using detrended fluctuation analysis (DFA).

MATERIALS AND METHODS

Participants

The sample included 36 neurotypical (NC) participants (mean ± SD: 34 ± 9 years old, 13 females, 1 left-handed), and 34 participants with a prior ADHD diagnosis (mean ± SD: 37 ± 9 years old, 19 females, 7 left-handed) recruited from a previous study [101], the University of Helsinki student body, and the local community through social media advertisement. There were no significant differences in age (Mann-Whitney U-test, $p = 0.084$) or gender

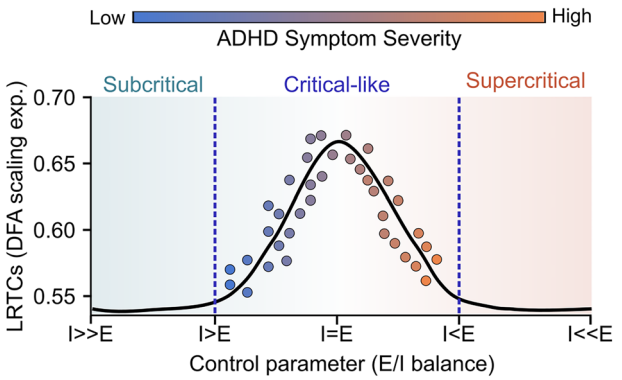


Fig. 1 Schematic of the hypothesis. Healthy human brains operate within the critical-like regime at the subcritical side near the critical peak. An individual's operating point, which regulates their position within the critical-like regime, is determined by control parameters, with the main control parameters being the excitation/inhibition (E/I) balance and AAS-based neuromodulation. Excessive excitation in ADHD shifts the operating point closer to the supercritical side of the critical regime, with this shift being dependent upon the extent of excitability. This shift towards the supercritical side of the critical-like regime predicts the severity of symptoms, with greater deviation from the critical peak corresponding to more severe symptoms.

(Chi-square test, $p = 0.097$) between the two cohorts. However, there were significantly more left-handed participants in the ADHD cohort (Chi-square test, $p = 0.019$).

The inclusion criteria for all participants were: aged 18–60 years, had normal or corrected to normal vision, and were compatible with MEG and MRI. Inclusion criteria for the ADHD cohort required an existing ADHD diagnosis made within the Finnish healthcare system and based on the International Classification of Diseases (ICD-10), as evaluated by medical professionals. Exclusion criteria included any comorbid psychiatric or neurological disease, substance abuse, or medications affecting the central nervous system. ADHD participants refrained from ADHD-specific medications 24 h before the MEG recordings. This study was conducted in compliance with the Declaration of Helsinki and approved by the Research Ethics Board at the Helsinki University Central Hospital. All participants gave written informed consent prior to participation.

Psychopathology

ADHD symptoms were assessed in all participants using the Barratt Impulsiveness Scale (BIS) [102] and Adult ADHD Self-Report Scale (ASRS) [103]; see Table S1 and Table S2. We first validated that the participants in the ADHD cohort exhibited clinical symptoms as measured by the two scales and that participants in the NC cohort had scores consistent for neurotypical populations. For the ADHD cohort, the mean and standard deviation (SD) were 81.10 ± 12.46 for BIS and 17.41 ± 3.75 for ASRS (Fig. 2E). For the NC cohort, total scores were 60.13 ± 9.79 for BIS and 9.71 ± 3.49 for ASRS, both of which were significantly lower than in the ADHD cohort (ASRS, Mann-Whitney U-test, $p = 5.2E\text{-}11$; BIS, Mann-Whitney U-test, $p = 7.6E\text{-}9$, Fig. 2E). Participants with symptoms highly consistent with ADHD were identified using the ASRS based on responses to six screening questions in Part A, with a score of four or more items marked as "Often" or "Very Often" serving as the cut-off. Three participants from the NC cohort fulfilled these screening criteria for ADHD and were excluded from all subsequent analyses, except for the correlation between neuronal LRTCs and ADHD symptoms.

Tasks and experiments

MEG data were collected during resting state (RS) and two visual CPTs: a Visual Threshold of Stimulus Detection Task (TSDT) [88] and a Go/NoGo task [69]. As reliable estimation of DFA exponents within an individual requires at least 10 min of data [88], we collected data over 25- and 17-min runs for TSDT and Go/NoGo, respectively. Tasks were conducted on either one or two days, with the task order counterbalanced across participants. Four participants performed only the TSDT and four performed only the Go/NoGo task, leaving $N = 62$ total participants who performed both tasks. Both tasks were presented onto a projector screen inside a magnetically shielded room during MEG recordings. Participants provided responses via a button press (dual handheld RESPONSEPixx/MRI).

Resting state

Before the task data collection, participants underwent 10 min of eyes-open resting state (RS) MEG recording, during which they fixated on a central cross. Data for RS was collected from $N = 36$ NC participants and $N = 34$ ADHD participants.

Visual threshold of stimulus detection task (TSDT)

Participants detected visual stimuli presented at their perceptual threshold, as described in [88] (Fig. 2A), with the task programmed and executed using MATLAB (MathWorks, Natick, MA, USA). The visibility of stimuli from slowly varying gradient noise was individually pre-calibrated to achieve a 50% detection rate using the adaptive QUEST algorithm (Table S1). Here, prolonged periods or 'streaks' of consecutive misses reflected lapses in sustained attention. Visual stimuli of two shapes (50% probability) were presented in any orientation with duration of 0.1 s with a diameter of 10° and with a random inter-stimulus interval (ISI) of 1.5–4.5 s. Each participant completed 500 stimulus trials over ~25 min.

Go/NoGo task

The Go/NoGo task was performed as in [69] using Presentation™ software (Neurobehavioral Systems, Inc., Albany, CA, USA). Participants responded as quickly as possible to Go stimuli (blue diamond) and refrained from responding to NoGo stimuli (yellow diamond) (Fig. 2B). Commission errors (false alarms) were erroneous responses to NoGo stimuli and constituted a measure of insufficient cognitive control. The stimuli were presented with a size of 1° for 0.1 s on a grey background (Fig. 2B). The Go (75%) and NoGo (25%) trials were randomly distributed in the stimulus stream with SOA of 1 s. Each participant completed 1000 trials over ~17 min.

Behavioral data analysis

Hit Rates (HRs) for TDST were the proportion of correct detection for responses at latencies 200–1500 ms. Seven participants from the NC cohort and five participants from the ADHD cohort with HR < 25% were excluded from the analysis leaving $N = 27$ ADHD and $N = 27$ NC participants. In the Go/NoGo task, HRs were computed for the correctly responded Go-trials ('Hits') and incorrectly responded NoGo-trials ('Commission errors') for responses within 150–800 ms from stimulus onset. The false alarm rate was computed as the number of incorrectly responded NoGo-trials divided by the total number of NoGo trials presented. Five participants from both the NC and ADHD cohorts with HR < 65% for the Go stimuli were excluded leaving $N = 28$ ADHD and $N = 28$ NC participants. Reaction time variability (RTV) was derived by computing standard deviations over the individual RTs in Go-trials. Behavioral LRTCs were computed over Hit and Miss time-series in TSDT as in [88] and in the Go/NoGo task for the RTs time-series as in [69], using Detrended Fluctuation Analysis (DFA) as in [85].

MEG and MRI recordings

MEG data (Elekta Neuromag TRIUX) were recorded at the BioMag laboratory in the HUS Medical Imaging Centre with a 1000 Hz sampling rate and 0.03–330 Hz online passband. Electrooculography data were recorded for ocular artifact removal. T1-weighted anatomical MRI scans for cortical surface reconstruction were obtained from every participant at a resolution of 1 ×1 x 1 mm (MP-RAGE) with a 1.5 T MRI scanner (Siemens, Germany).

MEG preprocessing, source analysis, and surface parcellations

Source reconstruction and data analysis followed previously published procedures [104–107]. Maxfilter software (Elekta Neuromag) was used to suppress extra-cranial noise and interpolate bad channels. Independent component analysis (ICA) (MATLAB) was used for removing ocular and cardiac artefacts, which were identified by correlating with a reference signal from the electrooculography (EOG) or the MEG magnetometers, respectively. ICA components with a high correlation were visually inspected before removal. MEG data were filtered using Morlet wavelets between 3–120 Hz with $m = 5$. Freesurfer was used for volumetric segmentation of the MRI data, surface reconstruction, flattening, and creating the cortical parcellation using the Destrieux atlas. 400 parcels were obtained by iteratively splitting the largest parcels, resulting in roughly equal-sized parcels [108, 109]. Source modelling was performed with MNE using noise-covariance matrices with a regularization constant of 0.05 computed from filtered (200–250 Hz) baseline data (-0.75–0.25 s). Source-space vertices were collapsed into the 400 parcels of the Destriux atlas using a fidelity-weighted collapse operator [110]. The 400 parcel parcellation was obtained by iteratively splitting the largest parcels of the Destriux atlas along their most elongated axis using the same parcel-wise splits for all participants and ensures high spatial resolution. However, as there might be considerable intersubject anatomical variability, we collapsed these to a coarser 200-parcel parcellation before statistical analysis.

Analysis of LRTCs from neuronal MEG Data

All data-analyses were carried out in a data-driven manner analysing data for each wavelet frequency and for each parcel. LRTCs of oscillation amplitude fluctuations were estimated with DFA [88, 111], which yields the scaling exponent β. This exponent is a measure of temporal clustering capable of predicting fluctuations in a one-dimensional time series over a long temporal range. β values between 0.5 and 1 indicate strong temporal dependencies, which is an indication of criticality, while values closer to 0.5 are associated with uncorrelated noise. DFA exponents were computed per cortical parcel on amplitude envelopes of filtered parcel time-series, by segmenting data into time windows Δt from 1–225 s. This range was chosen following prior art [69, 91, 112, 113] on estimating LRTCs and to ensure that the largest window was below 25% of the total recording duration, as such long windows make slope estimation unstable. Each segment of integrated data was then locally fitted.

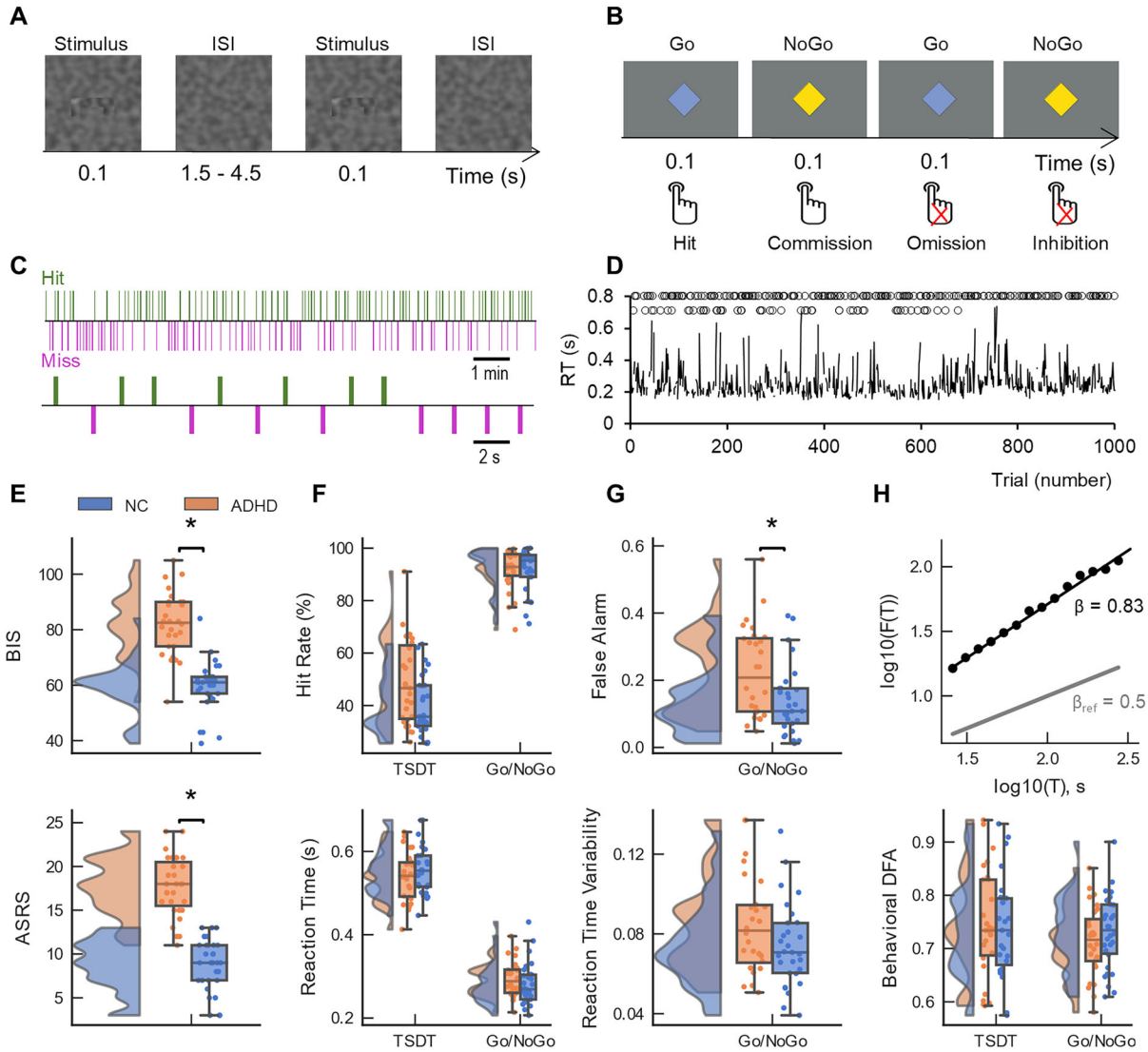


Fig. 2 Task schematics and behavioral data. Schematics of (**A**) Threshold of Stimulus Detection Task (TSDT) and (**B**) Go/NoGo experiments. **C** A short snapshot period of Hit-Miss time-series of a representative participant in TSDT. **D** Reaction Time (RT) series of a representative participant for each trial in Go/NoGo. Circles in the lower line above the time-series represent omission errors and circles in the upper line are trials with successful inhibition. **E** Distribution of BIS and ASRS scores for the ADHD (orange) and NC (blue) cohort. The box extends from the lower quartile (Q1, 25th percentile) to the upper quartile (Q3, 75th percentile). The line at the center of the boxplot indicates the median and the whispers represent the range of the data. The black bar above the boxplots with asterisk denotes significant differences between the ADHD and NC cohorts (Mann-Whitney U-test, $p < 0.05$). **F** Distribution of Hit rate (HR), and RT distributions separately for TSDT and Go/NoGo tasks. **G** Same as **F** but for **F**A rate and RTV (**H**) Top: the fitting for the behavioral DFA exponents in a representative subject from the ADHD cohort for the TSDT task. Black line indicates the fitting and the gray line the fitting for the null hypothesis. Bottom: behavioral DFA of the NC and ADHD cohorts.

Statistical analysis

Non-parametric Mann-Whitney U-test was used to test differences in behavioral performance between the NC and ADHD cohorts. The correlation between behavioral task performance with ASRS and BIS scores were assessed with Spearman's ranked correlation test.

Before statistical testing, the 400 parcel MEG data were collapsed into 200 parcels to improve statistical stability by reducing the effects of inter-subject variability [105]. Within-group differences between task-state and resting-state were obtained with Wilcoxon signed-ranked test separately for each frequency and parcel. Group differences were obtained using Welch's *t*-test. Post-hoc analysis for the correlations between clinical scores and neuronal and behavioral scaling laws were estimated with Spearman rank correlation and quadratic correlations tests. Effect size estimates were obtained using Cohen's *d*. Due to the strong dependencies of source-reconstructed MEG data across cortical parcels, standard FDR procedures severely overestimate the degrees of freedom, leading to an inflation of false negatives. Multiple comparisons were therefore controlled by the following approach [114] used also in prior studies [104–107]. First, we removed 5% of the least significant parcels observed at $\alpha = 0.05$. To remove remaining false positive observations, we estimated a threshold Q to define the proportion of significant observations that could thereafter arise by chance in any of the wavelet frequencies.

Data/code availability statement

Raw electrophysiological data cannot be shared publicly due to regulations imposed by the Ethical Committees but can be shared for collaborative efforts upon request. All python code used in this work to run the analyses and create the final figures can be found at https://github.com/palvalab/ADHD.

RESULTS

We assessed behavioral measures using the TSDT (Fig. 2A) and Go/NoGo (Fig. 2B) tasks by analyzing the behavioral time-series data

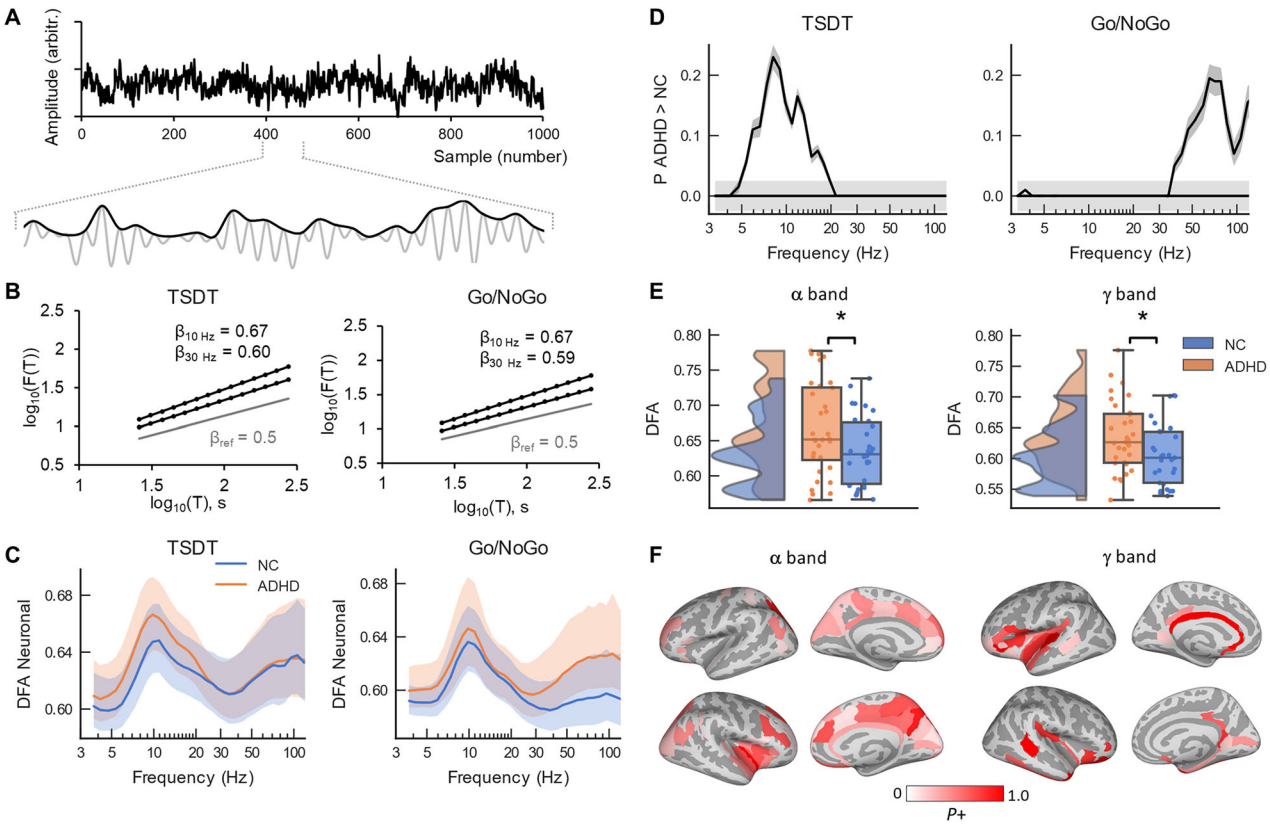


Fig. 3 Differential modulations of neuronal DFA exponents in ADHD and NC cohorts at the whole-brain level. A Example of unfiltered neuronal time-series (top) and filtered oscillation amplitude time-series (bottom, gray trace) with the amplitude envelope (bottom, black trace) (**B**) DFA exponents extracted from oscillation amplitude envelope for a representative participant during TSDT (Threshold of Stimulus Detection Task) and Go/NoGo tasks. The scaling exponent β for 10 Hz and 30 Hz filtered data (black lines) and for uncorrelated noise (gray line). **C** Group-level mean DFA exponents averaged over all parcels as a function of frequency for ADHD (orange) and NC (blue) cohorts during both tasks. Shading shows 95% confidence intervals. **D** Group-level differences in the DFA exponents between NC and ADHD cohorts estimated separately for each cortical parcel (Welch *t*-test, $p < 0.05$, FDR corrected). The *y*-axis shows the fraction of cortical parcels (*P*) in which the difference was significant. DFA exponents were significantly greater in ADHD compared to NC in the α-band (8–13 Hz) for TSDT and in the γ-band (35–65 Hz) for Go/NoGo. **E** Distribution of individual DFA exponents averaged over significant frequencies and parcels from D for the α-band in TSDT and the γ-band in Go/NoGo. Boxplots were drawn using the same convention as in Fig. 2. The bar shows statistical significance between NC and ADHD (two-tailed independent measures t-test, $p < 0.05$). **F** Cortical regions in which the differences in DFA exponents were observed in the α-band in TSDT and in the γ-band for Go/NoGo. The red color indicates the fraction of time-frequency elements ($P+$) that were significantly increased in ADHD compared to NC.

(Fig. 2C–D). As the TSDT task was pre-calibrated to a 50% stimulus-detection rate (Hit Rate, HR), as expected, the between-group differences in HRs were not significant (Fig. 2F) (NC 40.26 ± 11.38% (mean ± SD), ADHD 48.8 ± 16.25%, Mann-Whitney U-test, $p = 0.054$) nor were the RTs (NC 0.56 ± 0.058 s, ADHD 0.54 ± 0.059 s, Mann-Whitney U-test, $p = 0.35$). In the Go/NoGo task, neither HRs (NC 91.8 ± 8.17%, ADHD 91.9 ± 7.5%, Mann-Whitney U-test, $p = 0.86$), RTs (NC 0.28 ± 0.05 s, ADHD 0.29 ± 0.042 ms, Mann-Whitney U-test, $p = 0.16$), nor reaction time variability (RTV) (NC 0.074 ± 0.021 s, ADHD 0.084 ± 0.024 s, Mann-Whitney U-test, $p = 0.098$) were significantly different between the groups (Fig. 2F, G). However, the false alarm (FA) rate was larger for the ADHD cohort compared to the NC cohort (NC 0.14 ± 0.1, ADHD 0.22 ± 0.13, Mann-Whitney U-test, $p = 0.018$, Fig. 2G), as found previously [115, 116].

We then assessed LRTCs in the behavioral Hit Miss times-series (Fig. 2C) and RT time-series (Fig. 2D) data for the TSDT and Go/NoGo tasks, respectively, using DFA (Fig. 2H). DFA exponents did not differ between NC and ADHD cohorts for TSDT (0.74 ± 0.093 and 0.75 ± 0.1 respectively, Mann-Whitney U-test, $p = 0.78$, Fig. 2H), or the Go/NoGo task (0.73 ± 0.069 in the NC cohort and 0.71 ± 0.065 in the ADHD cohort, Mann-Whitney U-test, $p = 0.34$).

Neuronal LRTCs are stronger in ADHD than in NC cohort

Oscillation amplitude envelopes were extracted from Morlet-wavelet filtered source-reconstructed MEG data (Fig. 3A) and DFA exponents were used to assess the LRTCs in the oscillation amplitudes (Fig. 3B). The mean DFA obtained by averaging data across all parcels peaked in the α-band (8 − 13 Hz) in both tasks and cohorts (Fig. 3C). Consistent with this, DFA exponents were smaller for NC than for the ADHD cohort also at the parcel-level in the α-band (8 − 13 Hz) in the TSDT task and in the gamma-band (γ, 35 − 65 Hz) in the Go/NoGo task (Fig. 3D) (Welch's *t*- test, $p < 0.05$, FDR corrected). To assess the robustness of these differences *post hoc*, we averaged the DFA exponents across the significant frequencies. DFA exponents were significantly larger for ADHD than NC in both tasks (Fig. 3E) with moderate effect sizes of $d = 0.54$ for TSDT and $d = 0.57$ for Go/NoGo. Larger DFA exponents in the ADHD cohort were localized to the temporal, occipital and prefrontal cortices in TSDT (Fig. 3F). In Go/NoGo, differences in DFA exponents were observed in the occipito-temporal, visual, and cingulate cortices. The α-band and γ-band effects remained significant after controlling for age in the two cohorts using ANCOVA with age as a covariate (Fig. S1). We further investigated whether

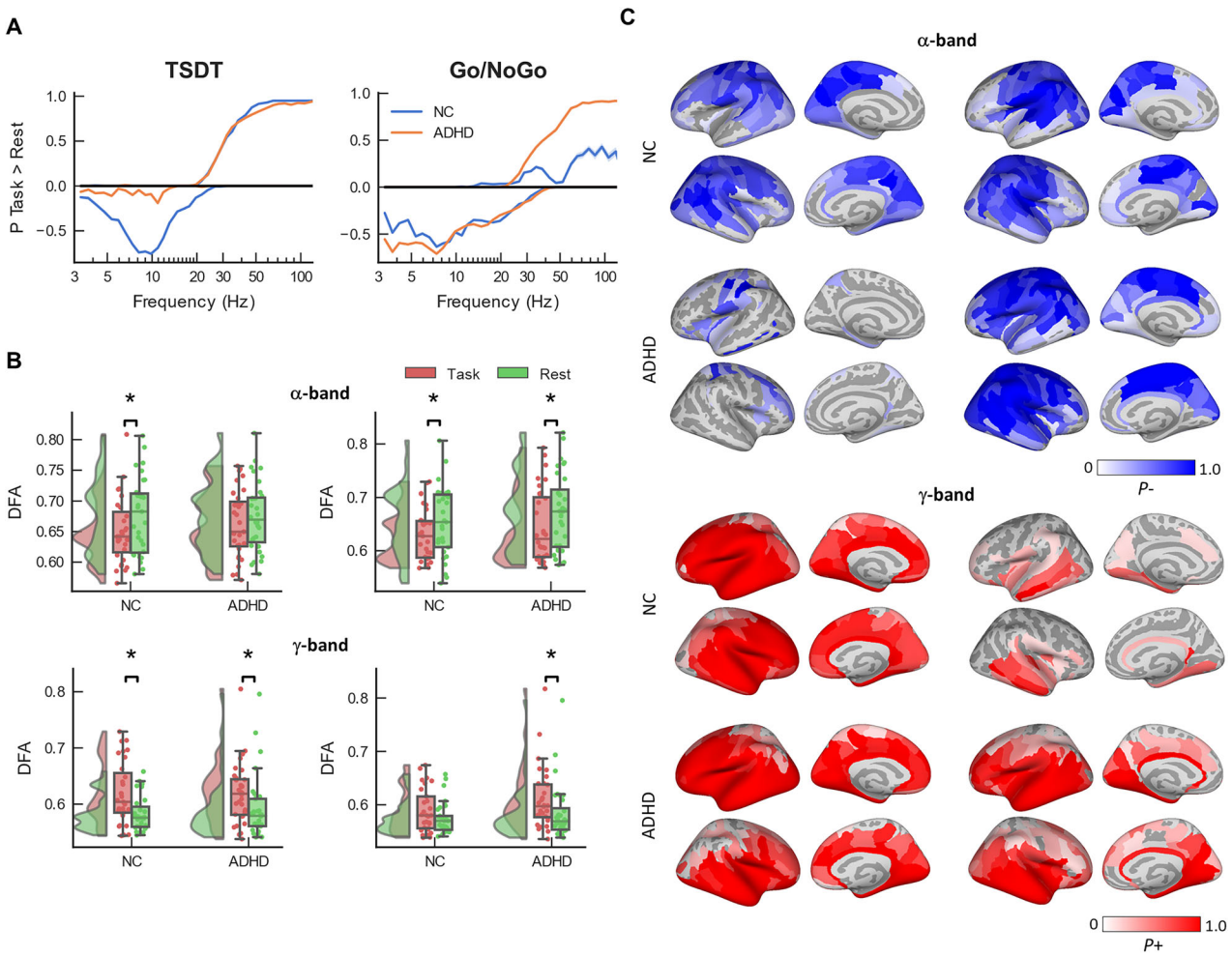


Fig. 4 Task dependent modulations of neuronal DFA exponents. A Differences in DFA exponents between task and rest for the NC (blue) and ADHD (orange) cohorts (Wilcoxon signed rank test, $p < 0.05$, FDR corrected). Positive values indicate the proportion of cortical parcels where DFA exponents were larger during the Task compared to Rest ($P+$), while the negative values indicate the proportion of parcels where DFA exponents were larger during Rest than Task (P-). Axis and shading as in Fig. 3D. **B** Distribution of individual DFA exponents for Task and Rest, separately for the NC and ADHD cohorts, in the α-band (8–13 Hz) (top) and γ-band (35–65 Hz) (bottom). Individual DFA exponents were computed from the average of all cortical parcels at the selected frequency range. The black bar with asterisk indicates significant differences in DFA exponents between Task and Rest (Wilcoxon signed-rank test, $p < 0.01$). **C** Cortical regions in which the DFA exponents were reduced in α-band by task performance (top) and increased in the γ-band by task performance (bottom). The red and blue colors indicate the fraction of time-frequency elements that were significantly increased ($P+$) or suppressed (P-), respectively.

differences in DFA exponents reflect signal-to-noises differences caused by differences in oscillation amplitudes between the two cohorts (Fig. S2) but found no significant differences in the mean parcel amplitudes between the cohorts (Welch t-test, $p < 0.05$, FDR corrected).

ADHD cohort shows different task-dependent modulation of LRTCs

Transitioning from a passive state (resting state) to an active task (TSDT / Go/NoGo) requires the engagement of attentional and executive networks. We therefore investigated task-related activation in the DFA exponents. In the NC cohort, DFA exponents were suppressed in the α-band (8–13 Hz) and increased in the γ-band (35 − 65 Hz) in task compared to the RS (Fig. 4A) (Wilcoxon signed rank test, $p < 0.05$, FDR corrected). However, in the ADHD cohort, there was only a weak suppression in the α-band DFA exponents in TSDT, and a robust increase in γ-band DFA exponents in Go/NoGo during task compared to RS (Fig. 4A).

To assess the reliability of these effects, we averaged individual DFA exponents in the α-band and γ-band for Task and Rest (Fig. 4B). The α-band DFA exponents were significantly higher during Rest than Task for the NC (moderate effect, $d = 0.43$) cohort in TSDT and both the NC (moderate effect, $d = 0.42$) and ADHD (moderate effect, $d = 0.41$) cohorts in Go/NoGo (Wilcoxon signed-rank test, $p < 0.01$). This difference was not significant for the ADHD cohort in the TSDT task (small effect, $d = 0.23$) For the γ-band, significant task modulation was observed for the ADHD cohort in TSDT (moderate effect, $d = 0.47$) and Go/NoGo (moderate effect, $d = 0.47$), but for the NC cohort in only TSDT (large effect, $d = 0.80$). This difference was not significant for the NC cohort in Go/NoGo (small effect, $d = 0.39$).

The α-band suppression of DFA exponents was widespread in the NC cohort for both tasks and found predominantly in the visual and somatomotor systems (Fig. 4C). This pattern was also observed in the ADHD cohort for Go/NoGo but not for TSDT, where only a few frontal regions exhibited any significant task modulations. The γ-band DFA exponents increased in nearly all brain regions for TSDT and in the ventral visual cortex and temporal regions for Go/NoGo.

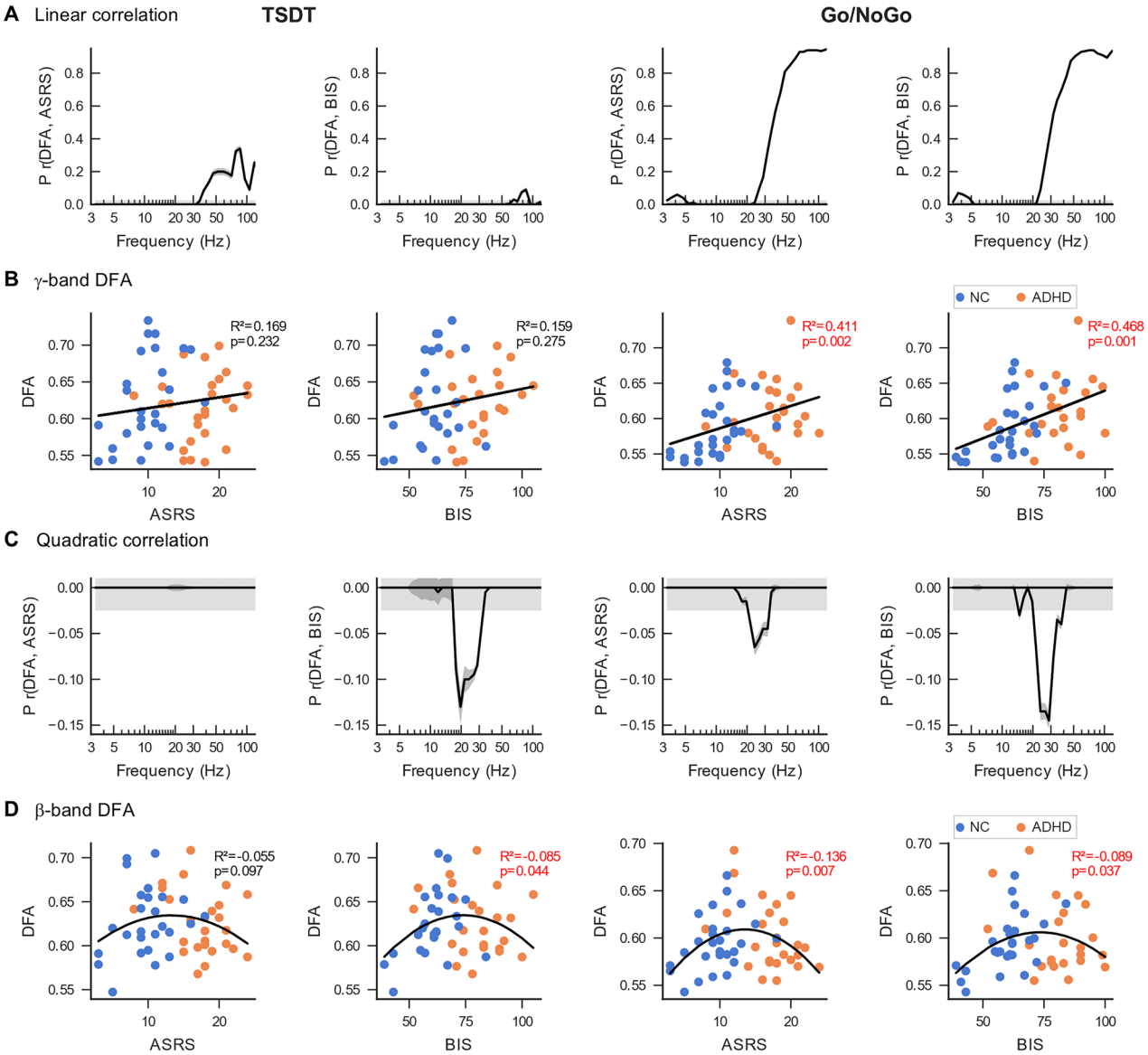


Fig. 5 ADHD symptom scores predict neuronal LRTCs with an inverted U-shaped curve. A Linear correlation of neuronal DFA exponents with total ASRS and BIS scores (Spearman rank correlation test, $p < 0.05$, FDR corrected) for TSDT and Go/NoGo tasks. The *y*-axis shows the fraction of cortical parcels (*P*) where a significant correlation was observed. Participants from both the NC and ADHD cohorts were included. DFA exponents were significantly correlated with BIS and ASRS symptom scores in the high frequencies (30-100 Hz). **B** Scatter plots for DFA exponents averaged over the γ-band (47-52 Hz) with BIS and ASRS scores. Data is plotted for the TSDT and the Go/NoGo tasks and includes all participants from the ADHD (orange dots) and NC (blue dots) cohorts. **C** Same as in **A** but for the quadratic correlation between DFA exponents and ASRS or BIS scores. **D** Same as in **B** but for DFA exponents averaged over the β-band (22-24 Hz).

Neuronal LRTCs are correlated with ADHD symptoms

We then quantified whether these LRTC differences would predict ADHD symptom score and severity using combined data across the NC and ADHD cohorts. We analyzed both linear and quadratic correlations as LRTCs show a non-linear dependence on the genetic polymorphism of the neuromodulatory genes [91] and neurotransmitter levels and further because ADHD characteristics can also be positive behavioral features [14–16] to some extent.

DFA exponents in the high frequencies ($30 - 100$ Hz) were positively linearly correlated with ASRS and BIS scores (Spearman's rank correlation coefficient, $p < 0.05$, FDR corrected) (Fig. 5A), with this effect being more robust for the Go/NoGo than TSDT. A *post-hoc* correlation test (Spearman's rank correlation coefficient, $p < 0.05$) between the individual mean DFA exponents in the gamma frequency ($47 - 52$ Hz) and the ASRS and BIS scores revealed a significant positive linear correlation across individuals, this being robust for the Go/NoGo task (ASRS, $R^2 = 0.41$, $p = 0.002$; BIS, $R^2 = 0.47$, $p = 0.001$) (Fig. 5B).

As LRTCs peak at criticality, they may exhibit a quadratic relationship with symptoms if the symptoms are associated with operating point shifts across the peak of the critical regime. We estimated the quadratic DFA-symptom correlations for the combined NC-ADHD cohort with the linear component regressed out (Fig. 5C). In both tasks, β-band DFA exponents were negatively quadratically correlated with BIS (TSDT, $R^2 = -0.085$, $p = 0.044$; Go/NoGo, $R^2 = -0.089$, $p = 0.037$) and in the Go/NoGo also with ASRS scores ($R^2 = -0.14$, $p = 0.007$) (Partial-quadratic correlation test, $p < 0.05$, FDR corrected). These quadratic correlations across subjects were confirmed with a *post-hoc* test (Partial-quadratic correlation test, $p < 0.05$) using individual mean DFA exponents

averaged over all cortical parcels at the peak correlation frequency (22 − 24 Hz) (Fig. 5D).

DISCUSSION

Here, we investigated whether LRTC would differ between ADHD and healthy control cohorts as well as whether strength of LRTCs as measured with DFA scaling exponents would be correlated with the symptom severity. We show that ADHD is associated with increased LRTCs between 3-30 Hz band in TSDT and in 30-100 Hz band in the Go-NoGo task, with these ADHD-related deviations being associated with differential rest-vs-task modulation. Further, we show that LRTCs deviations are correlated with symptom severity in a frequency-dependent manner. While several converging lines of evidence indicate a shift towards elevated excitability in ADHD, the mechanisms translating these factors into systems-level brain dynamics have remained unclear. We propose that the frequency and task dependent differences can be interpreted with the extended criticality [61, 63, 64] and/or quasicriticality [67] frameworks, in which individual operating points can dynamically move within the regime to adjust operation according to the task needs. This framework predicts that increased excitation in ADHD would move the individual operating points towards criticality or supercriticality. In our previous work, we showed that healthy individuals operate at the subcritical side of the extended critical regime whereby α- and γ-band oscillations operated closest to the critical point [61]. Here we show the presence of frequency-specific deviances of LRTCs and their task-dependent changes in relation to ADHD symptoms suggesting that ADHD symptoms are consistent with circuit-specific changes in brain operating points in the critical state space. Moreover, the opposing downregulation of 3-30 Hz and upregulation of 20-100 Hz oscillations' "criticality" is in line with the flexible dynamic control of individual operating points by behavioral demands. The present findings provide a plausible systems-level interpretation for how these sub-second synaptic- and micro-circuit-level characteristics of ADHD may be translated into the excessive multi-second and -minute cognitive and behavioral fluctuations that are pervasive in ADHD psychopathology.

ADHD is often characterized by increased RTV on longer timescales in CPTs [117], which have been proposed to reflect deficits in top-down effortful control or arousal [118, 119]. However, we did not find any differences in RTVs between the cohorts. Even though RTV is an endophenotype of ADHD, recent observations highlight the complexity of this effect. First, the RTV has been shown to be pronounced under high cognitive load [120], but in the Go/NoGo task, the cognitive load was small. Second, cognitive and perceptual loads influence differentially RTV in ADHD and controls participants [121] which may also partially explain the null findings of RTV in the present study. These effects may explain the lack of RTV effect in the current study. Third, increased RTV in ADHD has been proposed to be associated with higher arousal [80] while the experimental situation with MEG scanning could have led to overall higher arousal levels also in the HC cohort and thus to small group differences. In contrast, FA rate was larger in the ADHD group as found earlier. These results are consistent with the possibility that ADHD patients might engage compensatory processes for the task performance.

While healthy controls had downregulation in the 3-30 Hz band LRTCs during the TSDT task, this was only weakly present in the ADHD cohort. In contrast, ADHD was associated with excessive upregulation in the 20-100 Hz band during the Go/NoGo task compared to the healthy controls. The Go/NoGo task requires cognitive control, response inhibition, and motor control, of which deficits are typically associated with ADHD [1] and localized to the PFC and PPC cortices associated with attention and executive functions [33, 122]. In contrast, TSDT task requires sustained visual perception modulated by top-down attention that is associated with tonic-like modulations of local [33, 123] and inter-areal α- [104, 124] as well as γ-band oscillations [125, 126]. Increased LRTCs in the Go/NoGo task were thus in line with findings of previous studies, which have shown cognitive control deficits [9, 127] as well as hyperconnectivity within DAN (Dorsal Attention Network) and between DAN and VAN (Ventral Attention Network) in ADHD [128]. Excessively increased γ-band LRTCs could thus reflect compensatory mechanisms to overcome the deficits in sustaining attention upon task demands [129, 130]. Differences in LRTCs between ADHD and NC cohorts could also further reflect prolonged brain maturation [131], which is a characteristic of ADHD [132, 133].While perceptual fluctuations are not a core deficiency of ADHD, we postulate that, in TSDT, decreased task-dependent modulation of LRTCs could reflect differences in sustained attentional fluctuations and mind wandering [134]. Further, perceptual load may be beneficial to cognitive performance in ADHD [135], because it shifts the neuronal processing from top-down to bottom-up driven [136]. Task differences between Go/NoGo and TSDT tasks are in line with the differential influence of cognitive load and perceptual load both influence task performance in ADHD and healthy controls [120].

Elevated LRTCs observed in ADHD are indicative of shifts in the brain's operating point from the subcritical side towards more excitation-dominated supercritical states within the critical regime. As E/I balance and AAS modulation of E/I are key constructs for the biological control parameters determining this operating point, the shift observed in this study is congruent with several lines of evidence implicating excessive excitability and abnormal AAS regulation [78, 79, 82] through both elevated glutamatergic excitation and GABAergic inhibitory deficits [78, 79] as well as in norepinephrine (NE) and dopamine (DA) levels [80, 81] which together with diverse feedback mechanisms [76], may contribute to the complex frequency and task specific modulations observed in the present study.

Importantly, ADHD symptom severity in ASRS and BIS scores were predicted by individual variability in LRTCs. This is in line with the recent frameworks that conceptualize mental disorders as a spectrum of symptoms suggesting an underlying continuum of increased dysfunction [137–139]. In the γ-band, these correlations were predicted by a linear relationship while in β-band by quadratic relationship. This indicates that different frequencies associated with multiple distinct spatio-temporal circuitries are associated with the emergence of ADHD symptoms in a different way in line with diverse biological foundations of brain disorder symptoms. Further, the spatial and frequency-wise variability of the correlations (allowing both linear and quadratic correlations to emerge) is in line with the extended brain criticality framework [61, 63, 64], whereby there is variability in the individual operating points in the critical state space emerging from the heterogeneity of the underlying structure. In line with γ-band LRTCs being modulated by the Go/NoGo task, only in this task were the γ-band LRTCs positively correlated with ASRS and BIS scores and hence, the most severe symptoms were associated with the largest LRTCs indicating their closeness to criticality. In contrast, in both tasks the β-band LRTCs were the strongest for the moderate BIS scores and in the Go/NoGo task also for the ASRS scores across the neurotypical and ADHD cohorts with inverted U-shaped (parabolic) correlations such that the largest LRTCs were associated with intermediate symptom scores, while conversely, low scores in neurotypical controls and high scores in the ADHD cohort were associated with smaller LRTCs. Overall, these results of correlations with LRTCs and symptom scores suggest that ADHD symptoms and their severity could be related to increases in excitation leading to shifts in the brain operating point from subcritical toward the super-critical phase. However, taking into account the limitations in the sample, other plausible mechanisms could also explain the results. Given that healthy control subjects and

frequencies operate mostly at the subcritical side, the small increases in excitability could move the operating point either to or near the critical transition point that is associated with high LRTCs and many functional benefits [52, 54, 55], while larger shifts in excitability would move the operating point to the supercritical side. This is associated with smaller LRTCs, excessive activity propagation and hyper-synchrony that are functionally detrimental and may be associated with emergent behavioral and cognitive dysfunction manifested as typical ADHD symptoms emerging as the progressive shift towards the supercritical side. Notably, these excitation dependent shifts are plausibly frequency dependent, yielding to the emergence of multiscale complex dynamics changes.

Importantly, operation at the critical-like regime is associated with beneficial neuronal dynamics [52, 54, 55], such as moderate levels of neuronal synchronization dynamics [48, 61] enhanced storage capacity [50], as well as beneficial behavioral performance, such as higher fluid intelligence [69, 140]. Interestingly, in our data, moderate ADHD characteristics associated with high beta-band LRTCs, could thus also be beneficial. These findings are in line with studies showing that mild ADHD is associated with traits such as hyper-focus on highly motivating tasks [14, 15], novelty-seeking [16], cognitive flexibility [141], and sensation-seeking [142], which are advantageous features in changing environments.

In conclusion, our finding supports emerging frameworks which suggest that mental health symptoms, here associated with ADHD, arise from a continuum of brain dysfunction [137]. We propose that the emergence of ADHD symptoms and their continuum across the population can be explained in the framework of complex systems dynamics. More precisely, our results support the idea that individual variability in ADHD symptoms reflects the variability of individual operating points – individual brain states - in the brain criticality framework.

REFERENCES

1. Faraone SV, Bellgrove MA, Brikell I, Cortese S, Hartman CA, Hollis C, et al. Attention-deficit/hyperactivity disorder. Nat Rev Dis Primers. 2024;10:11.
2. Nijmeijer JS, Minderaa RB, Buitelaar JK, Mulligan A, Hartman CA, Hoekstra PJ. Attention-deficit/hyperactivity disorder and social dysfunctioning. Clin Psychol Rev. 2008;28:692–708.
3. Ging-Jehli NR, Pine DS. From symptom-based heterogeneity to mechanism-based profiling in youth ADHD: the promise of computational psychiatry. Neuropsychopharmacology 2025;51:234–243. https://doi.org/10.1038/s41386-025-02254-5.
4. Karalunas SL, Nigg JT. Heterogeneity and subtyping in attention-deficit/hyperactivity disorder-considerations for emerging research using person-centered computational approaches. Biol Psychiatry. 2020;88:103–10.
5. Salum GA, Sato JR, Manfro AG, Pan PM, Gadelha A, do Rosário MC, et al. Reaction time variability and attention-deficit/hyperactivity disorder: is increased reaction time variability specific to attention-deficit/hyperactivity disorder? Testing predictions from the default-mode interference hypothesis. Atten Defic Hyperact Disord. 2019;11:47–58.
6. Kember J, Stepien L, Panda E, Tekok-Kilic A. Resting-state EEG dynamics help explain differences in response control in ADHD: Insight into electrophysiological mechanisms and sex differences. PLoS ONE. 2023;18:e0277382.
7. Tamm L, Dudley JA, Karalunas SL, Simon JO, Maloney TC, Atluri G, et al. Exploring the neural basis of reaction time variability in ADHD: The importance of examining data at the trial level. Neuroimage Rep. 2025;5:100263.
8. Kofler MJ, Rapport MD, Sarver DE, Raiker JS, Orban SA, Friedman LM, et al. Reaction time variability in ADHD: a meta-analytic review of 319 studies. Clin Psychol Rev. 2013;33:795–811.
9. Cai W, Warren SL, Duberg K, Pennington B, Hinshaw SP, Menon V. Latent brain state dynamics distinguish behavioral variability, impaired decision-making, and inattention. Mol Psychiatry. 2021;26:4944–57.
10. Forstmann BU, Ratcliff R, Wagenmakers E-J. Sequential sampling models in cognitive neuroscience: advantages, applications, and extensions. Annu Rev Psychol. 2016;67:641–66.
11. Huang-Pollock C, Ratcliff R, McKoon G, Shapiro Z, Weigard A, Galloway-Long H. Using the diffusion model to explain cognitive deficits in attention deficit hyperactivity disorder. J Abnorm Child Psychol. 2017;45:57–68.
12. Feldman JS, Huang-Pollock C. Slow drift rate predicts ADHD symptomology over and above executive dysfunction. Child Neuropsychol. 2021;27:834–55.
13. Epstein JN, Brinkman WB, Froehlich T, Langberg JM, Narad ME, Antonini TN, et al. Effects of stimulant medication, incentives, and event rate on reaction time variability in children with ADHD. Neuropsychopharmacology. 2011;36:1060–72.
14. Hupfeld KE, Abagis TR, Shah P. Living 'in the zone': hyperfocus in adult ADHD. Atten Defic Hyperact Disord. 2019;11:191–208.
15. Ashinoff BK, Abu-Akel A. Hyperfocus: the forgotten frontier of attention. Psychol Res. 2021;85:1–19.
16. Donfrancesco R, Di Trani M, Porfirio MC, Giana G, Miano S, Andriola E. Might the temperament be a bias in clinical study on attention-deficit hyperactivity disorder (ADHD)? novelty seeking dimension as a core feature of ADHD. Psychiatry Res. 2015;227:333–8.
17. Tolonen T, Leppämäki S, Roine T, Alho K, Tani P, Koski A, et al. Working memory related functional connectivity in adult ADHD and its amenability to training: A randomized controlled trial. Neuroimage Clin. 2024;44:103696.
18. Salmi J, Salmela V, Salo E, Mikkola K, Leppämäki S, Tani P, et al. Out of focus - brain attention control deficits in adult ADHD. Brain Res. 2018;1692:12–22.
19. Mizuno Y, Yamashita M, Shou Q, Hamatani S, Cai W. A brief review of MRI studies in patients with attention-deficit/hyperactivity disorder and future perspectives. Brain Dev. 2025;47:104340.
20. Pereira-Sanchez V, Castellanos FX. Neuroimaging in attention-deficit/hyperactivity disorder. Curr Opin Psychiatry. 2021;34:105–11.
21. Grimm O, van Rooij D, Hoogman M, Klein M, Buitelaar J, Franke B, et al. Transdiagnostic neuroimaging of reward system phenotypes in ADHD and comorbid disorders. Neurosci Biobehav Rev. 2021;128:165–81.
22. Lau-Zhu A, Fritz A, McLoughlin G. Overlaps and distinctions between attention deficit/hyperactivity disorder and autism spectrum disorder in young adulthood: Systematic review and guiding framework for EEG-imaging research. Neurosci Biobehav Rev. 2019;96:93–115.
23. Gamma A, Kara O. Event-related potentials for diagnosing children and adults with ADHD. J Atten Disord. 2020;24:1581–7.
24. Johnstone SJ, Barry RJ, Clarke AR. Ten years on: a follow-up review of ERP research in attention-deficit/hyperactivity disorder. Clin Neurophysiol. 2013;124:644–57.
25. Michelini G, Salmastyan G, Vera JD, Lenartowicz A. Event-related brain oscillations in attention-deficit/hyperactivity disorder (ADHD): A systematic review and meta-analysis. Int J Psychophysiol. 2022;174:29–42.
26. Hasler R, Perroud N, Meziane HB, Herrmann F, Prada P, Giannakopoulos P, et al. Attention-related EEG markers in adult ADHD. Neuropsychologia. 2016;87:120–33.
27. Marquardt L, Eichele H, Lundervold AJ, Haavik J, Eichele T. Event-related-potential (ERP) correlates of performance monitoring in adults with attention-deficit hyperactivity disorder (ADHD). Front Psychol. 2018;9:485.
28. Kaiser A, Aggensteiner P-M, Baumeister S, Holz NE, Banaschewski T, Brandeis D. Earlier versus later cognitive event-related potentials (ERPs) in attention-deficit/hyperactivity disorder (ADHD): A meta-analysis. Neurosci Biobehav Rev. 2020;112:117–34.
29. Dallmer-Zerbe I, Popp F, Lam AP, Philipsen A, Herrmann CS. Transcranial alternating current stimulation (tACS) as a tool to modulate P300 amplitude in attention deficit hyperactivity disorder (ADHD): Preliminary findings. Brain Topogr. 2020;33:191–207.
30. Johnstone SJ, Barry RJ, Markovska V, Dimoska A, Clarke AR. Response inhibition and interference control in children with AD/HD: a visual ERP investigation. Int J Psychophysiol. 2009;72:145–53.
31. Palva S, Palva JM. Functional roles of alpha-band phase synchronization in local and large-scale cortical networks. Front Psychol. 2011;2:204.
32. Miller EK, Buschman TJ. Cortical circuits for the control of attention. Curr Opin Neurobiol. 2013;23:216–22.
33. Fiebelkorn IC, Kastner S. Functional specialization in the attention network. Annu Rev Psychol. 2020;71:221–49.
34. Jensen O. Distractor inhibition by alpha oscillations is controlled by an indirect mechanism governed by goal-relevant information. Commun Psychol. 2024;2:1–11.
35. Lenartowicz A, Lu S, Rodriguez C, Lau EP, Walshaw PD, McCracken JT, et al. Alpha desynchronization and frontoparietal connectivity during spatial working memory encoding deficits in ADHD: A simultaneous EEGfMRI study. Neuroimage Clin. 2016;11:210–23.
36. Cowley BU, Juurmaa K, Palomäki J. Reduced power in fronto-parietal theta EEG linked to impaired attention-sampling in adult ADHD. eNeuro. 2022;9:ENEURO.0028–21.2021.
37. Kiiski H, Bennett M, Rueda-Delgado LM, Farina FR, Knight R, Boyle R, et al. EEG spectral power, but not theta/beta ratio, is a neuromarker for adult ADHD. Eur J Neurosci. 2020;51:2095–109.

38. Debnath R, Miller NV, Morales S, Seddio KR, Fox NA. Investigating brain electrical activity and functional connectivity in adolescents with clinically elevated levels of ADHD symptoms in alpha frequency band. Brain Res. 2021;1750:147142.
39. Mazaheri A, Fassbender C, Coffey-Corina S, Hartanto TA, Schweitzer JB, Mangun GR. Differential oscillatory electroencephalogram between attention-deficit/hyperactivity disorder subtypes and typically developing adolescents. Biol Psychiatry. 2014;76:422–9.
40. Vera JD, Freichel R, Michelini G, Loo SK, Lenartowicz A. A network approach to understanding the role of executive functioning and alpha oscillations in inattention and hyperactivity-impulsivity symptoms of ADHD. J Atten Disord. 2024;28:1357–67.
41. Vollebregt MA, Zumer JM, Ter Huurne N, Buitelaar JK, Jensen O. Posterior alpha oscillations reflect attentional problems in boys with attention deficit hyperactivity disorder. Clin Neurophysiol. 2016;127:2182–91.
42. Mazzetti C, Gonzales Damatac C, Sprooten E, Ter Huurne N, Buitelaar JK, Jensen O. Dorsal-to-ventral imbalance in the superior longitudinal fasciculus mediates methylphenidate's effect on beta oscillations in ADHD. Psychophysiology. 2022;59:e14008.
43. McLoughlin G, Gyurkovics M, Palmer J, Makeig S. Midfrontal theta activity in psychiatric illness: An index of cognitive vulnerabilities across disorders. Biol Psychiatry. 2022;91:173–82.
44. Lenartowicz A, Loo SK. Use of EEG to diagnose ADHD. Curr Psychiatry Rep. 2014;16:498.
45. Vainieri I, Michelini G, Adamo N, Cheung CHM, Asherson P, Kuntsi J. Event-related brain-oscillatory and ex-Gaussian markers of remission and persistence of ADHD. Psychol Med. 2022;52:352–61.
46. Smit D, Trevino L, Mohamed SMH, Enriquez-Geppert S. Theta power and functional connectivity as neurophysiological markers of executive functions in individuals with cognitive complaints in daily life. Biol Psychol. 2023;178:108503.
47. O'Byrne J, Jerbi K. How critical is brain criticality?. Trends Neurosci. 2022;45:820–37.
48. Palva S, Palva JM. Roles of brain criticality and multiscale oscillations in temporal predictions for sensorimotor processing. Trends Neurosci. 2018;41:729–43.
49. He BJ, Zempel JM, Snyder AZ, Raichle ME. The temporal structures and functional significance of scale-free brain activity. Neuron. 2010;66:353–69.
50. Cocchi L, Gollo LL, Zalesky A, Breakspear M. Criticality in the brain: A synthesis of neurobiology, models and cognition. Prog Neurobiol. 2017;158:132–52.
51. Kello CT, Brown GDA, Ferrer-I-Cancho R, Holden JG, Linkenkaer-Hansen K, Rhodes T, et al. Scaling laws in cognitive sciences. Trends Cogn Sci. 2010;14:223–32.
52. Shew WL, Plenz D. The functional benefits of criticality in the cortex. Neuroscientist. 2013;19:88–100.
53. Chialvo DR. Emergent complex neural dynamics. Nat Phys. 2010;6:744–50.
54. Kinouchi O, Copelli M. Optimal dynamical range of excitable networks at criticality. Nature Physics. 2006;2:348–51.
55. Lotfi N, Feliciano T, Aguiar LAA, Silva TPL, Carvalho TTA, Rosso OA, et al. Statistical complexity is maximized close to criticality in cortical dynamics. Phys Rev E. 2021;103:012415.
56. Hengen KB, Shew WL. Is criticality a unified set-point of brain function? Neuron. 2025;113:2582–98.
57. Villegas P, Moretti P, Muñoz MA. Frustrated hierarchical synchronization and emergent complexity in the human connectome network. Sci Rep. 2014;4:5990.
58. Diachenko M, Sharma A, Smit DJA, Mansvelder HD, Bruining H, de Geus E, et al. Functional excitation-inhibition ratio indicates near-critical oscillations across frequencies. Imaging Neurosci (Camb). 2024;2:imag-2-00318 https://doi.org/10.1162/imag_a_00318.
59. Beggs JM. The criticality hypothesis: how local cortical networks might optimize information processing. Philos Trans A Math Phys Eng Sci. 2008;366:329–43.
60. Amil AF, Verschure PFMJ. Supercritical dynamics at the edge-of-chaos underlies optimal decision-making. J Phys Complex. 2021;2:045017.
61. Fuscà M, Siebenhühner F, Wang SH, Myrov V, Arnulfo G, Nobili L, et al. Brain criticality predicts individual levels of inter-areal synchronization in human electrophysiological data. Nat Commun. 2023;14:4736.
62. Xu L, Feng J, Yu L. Avalanche criticality in individuals, fluid intelligence, and working memory. Hum Brain Mapp. 2022;43:2534–53.
63. Moretti P, Muñoz MA. Griffiths phases and the stretching of criticality in brain networks. Nat Commun. 2013;4:2521.
64. Muñoz MA, Juhász R, Castellano C, Odor G. Griffiths phases on complex networks. Phys Rev Lett. 2010;105:128701.
65. Deco G, Kringelbach ML, Arnatkeviciute A, Oldham S, Sabaroedin K, Rogasch NC, et al. Dynamical consequences of regional heterogeneity in the brain's transcriptional landscape. Sci Adv. 2021;7:eabf4752.
66. Demirtaş M, Burt JB, Helmer M, Ji JL, Adkinson BD, Glasser MF, et al. Hierarchical heterogeneity across human cortex shapes large-scale neural dynamics. Neuron. 2019;101:1181–.e13.
67. Fosque LJ, Alipour A, Zare M, Williams-García RV, Beggs JM, Ortiz G. Quasicriticality explains variability of human neural dynamics across life span. Front Comput Neurosci. 2022;16:1037550.
68. Safavi S, Chalk M, Logothetis NK, Levina A. Signatures of criticality in efficient coding networks. Proc Natl Acad Sci USA. 2024;121:e2302730121 https://doi.org/10.1073/pnas.2302730121.
69. Simola J, Zhigalov A, Morales-Muñoz I, Palva JM, Palva S. Critical dynamics of endogenous fluctuations predict cognitive flexibility in the Go/NoGo task. Sci Rep. 2017;7:2909.
70. Müller PM, Miron G, Holtkamp M, Meisel C. Critical dynamics predicts cognitive performance and provides a common framework for heterogeneous mechanisms impacting cognition. Proc Natl Acad Sci USA. 2025;122:e2417117122.
71. Ribeiro TL, Jendrichovsky P, Yu S, Martin DA, Kanold PO, Chialvo DR, et al. Trial-by-trial variability in cortical responses exhibits scaling of spatial correlations predicted from critical dynamics. Cell Rep. 2024;43:113762.
72. van Nifterick AM, Mulder D, Duineveld DJ, Diachenko M, Scheltens P, Stam CJ, et al. Resting-state oscillations reveal disturbed excitation–inhibition ratio in Alzheimer's disease patients. Sci Rep. 2023;13:7419. https://doi.org/10.1038/s41598-023-33973-8.
73. Bruining H, Hardstone R, Juarez-Martinez EL, Sprengers J, Avramiea A-E, Simpraga S, et al. Measurement of excitation-inhibition ratio in autism spectrum disorder using critical brain dynamics. Sci Rep. 2020;10:9195.
74. Javed E, Suárez-Méndez I, Susi G, Román JV, Palva JM, Maestú F, et al. A shift toward supercritical brain dynamics predicts Alzheimer's disease progression. J Neurosci. 2025;45:e0688242024 https://doi.org/10.1523/JNEUROSCI.0688-24.2024.
75. Wang SH, Siebenhühner F, Arnulfo G, Myrov V, Nobili L, Breakspear M, et al. Critical-like brain dynamics in a continuum from second- to first-order phase transition. J Neurosci. 2023;43:7642–56.
76. Sohal VS, Rubenstein JLR. Excitation-inhibition balance as a framework for investigating mechanisms in neuropsychiatric disorders. Mol Psychiatry. 2019;24:1248–57.
77. Munn BR, Müller EJ, Wainstein G, Shine JM. The ascending arousal system shapes neural dynamics to mediate awareness of cognitive states. Nat Commun. 2021;12:6016.
78. Mamiya PC, Arnett AB, Stein MA. Precision medicine care in ADHD: the case for neural excitation and inhibition. Brain Sci. 2021;11:91.
79. Puts NA, Ryan M, Oeltzschner G, Horska A, Edden RAE, Mahone EM. Reduced striatal GABA in unmedicated children with ADHD at 7T. Psychiatry Res Neuroimaging. 2020;301:111082.
80. James S-N, Cheung CHM, Rijsdijk F, Asherson P, Kuntsi J. Modifiable arousal in attention-deficit/hyperactivity disorder and its etiological association with fluctuating reaction times. Biol Psychiatry Cogn Neurosci Neuroimaging. 2016;1:539–47.
81. Ulke C, Rullmann M, Huang J, Luthardt J, Becker G-A, Patt M, et al. Adult attention-deficit/hyperactivity disorder is associated with reduced norepinephrine transporter availability in right attention networks: a (S,S)-O-[11C] methylreboxetine positron emission tomography study. Transl Psychiatry. 2019;9:301.
82. del Campo N, Fryer TD, Hong YT, Smith R, Brichard L, Acosta-Cabronero J, et al. A positron emission tomography study of nigro-striatal dopaminergic mechanisms underlying attention: implications for ADHD and its treatment. Brain. 2013;136:3252–70.
83. Arnsten AFT. Guanfacine's mechanism of action in treating prefrontal cortical disorders: Successful translation across species. Neurobiol Learn Mem. 2020;176:107327.
84. Arnsten AFT, Rubia K. Neurobiological circuits regulating attention, cognitive control, motivation, and emotion: disruptions in neurodevelopmental psychiatric disorders. J Am Acad Child Adolesc Psychiatry. 2012;51:356–67.
85. Hardstone R, Poil S-S, Schiavone G, Jansen R, Nikulin VV, Mansvelder HD, et al. Detrended fluctuation analysis: A scale-free view on neuronal oscillations. Front Physiol. 2012;3:450 https://doi.org/10.3389/fphys.2012.00450.
86. Wilting J, Priesemann V. 25 years of criticality in neuroscience - established results, open controversies, novel concepts. Curr Opin Neurobiol. 2019;58:105–11.
87. Avramiea A-E, Masood A, Mansvelder HD, Linkenkaer-Hansen K. Long-range amplitude coupling is optimized for brain networks that function at criticality. J Neurosci. 2022;42:2221–33.
88. Palva JM, Zhigalov A, Hirvonen J, Korhonen O, Linkenkaer-Hansen K, Palva S. Neuronal long-range temporal correlations and avalanche dynamics are correlated with behavioral scaling laws. Proc Natl Acad Sci USA. 2013;110:3585–90.
89. Smit DJA, Linkenkaer-Hansen K, de Geus EJC. Long-range temporal correlations in resting-state alpha oscillations predict human timing-error dynamics. J Neurosci. 2013;33:11212–20.

90. Jones SA, Barfield JH, Norman VK, Shew WL. Scale-free behavioral dynamics directly linked with scale-free cortical dynamics. eLife. 2023;12:e79950 https://doi.org/10.7554/eLife.79950.
91. Simola J, Siebenhühner F, Myrov V, Kantojärvi K, Paunio T, Palva JM, et al. Genetic polymorphisms in COMT and BDNF influence synchronization dynamics of human neuronal oscillations. iScience. 2022;25:104985.
92. Montez T, Poil S-S, Jones BF, Manshanden I, Verbunt JPA, van Dijk BW, et al. Altered temporal correlations in parietal alpha and prefrontal theta oscillations in early-stage Alzheimer disease. Proc Natl Acad Sci USA. 2009;106:1614–9.
93. Nikulin VV, Jönsson EG, Brismar T. Attenuation of long-range temporal correlations in the amplitude dynamics of alpha and beta neuronal oscillations in patients with schizophrenia. Neuroimage. 2012;61:162–9.
94. Cruz G, Grent-'t-Jong T, Krishnadas R, Palva JM, Palva S, Uhlhaas PJ. Long range temporal correlations (LRTCs) in MEG-data during emerging psychosis: relationship to symptoms, medication-status and clinical trajectory. Neuroimage Clin. 2021;31:102722.
95. Linkenkaer-Hansen K, Monto S, Rytsälä H, Suominen K, Isometsä E, Kähkönen S. Breakdown of long-range temporal correlations in theta oscillations in patients with major depressive disorder. J Neurosci. 2005;25:10131–7.
96. Duncan NW, Hsu T-Y, Cheng PZ, Wang H-Y, Lee H-C, Lane TJ. Intrinsic activity temporal structure reactivity to behavioural state change is correlated with depressive symptoms. Eur J Neurosci. 2020;52:4840–50.
97. Wang SH, Arnulfo G, Nobili L, Myrov V, Ferrari P, Ciuciu P, et al. Neuronal synchrony and critical bistability: Mechanistic biomarkers for localizing the epileptogenic network. Epilepsia. 2024;65:2041–53. https://doi.org/10.1111/epi.17996.
98. Jia H, Yu D. Attenuated long-range temporal correlations of electrocortical oscillations in patients with autism spectrum disorder. Dev Cogn Neurosci. 2019;39:100687.
99. Damiani S, Scalabrini A, Gomez-Pilar J, Brondino N, Northoff G. Increased scale-free dynamics in salience network in adult high-functioning autism. Neuroimage Clin. 2019;21:101634.
100. Huang J, Ahlers E, Bogatsch H, Böhme P, Ethofer T, Fallgatter AJ, et al. The role of comorbid depressive symptoms on long-range temporal correlations in resting EEG in adults with ADHD. Eur Arch Psychiatry Clin Neurosci. 2022;272:1421–35.
101. Cowley B, Holmström É, Juurmaa K, Kovarskis L, Krause CM. Computer enabled neuroplasticity treatment: a clinical trial of a novel design for neurofeedback therapy in adult ADHD. Front Hum Neurosci. 2016;10:205.
102. Patton JH, Stanford MS, Barratt ES. Factor structure of the barratt impulsiveness scale. J Clin Psychol. 1995;51:768–74.
103. Kessler RC, Adler L, Ames M, Demler O, Faraone S, Hiripi E, et al. The World Health Organization adult ADHD self-report scale (ASRS): A short screening scale for use in the general population. Psychol Med. 2005;35:245–56.
104. Lobier M, Palva JM, Palva S. High-alpha band synchronization across frontal, parietal and visual cortex mediates behavioral and neuronal effects of visuospatial attention. Neuroimage. 2018;165:222–37.
105. Rouhinen S, Siebenhühner F, Matias Palva J, Palva S. Spectral and anatomical patterns of large-scale synchronization predict human attentional capacity. Cereb Cortex. 2020;30:5293–308.
106. Hirvonen J, Monto S, Wang SH, Palva JM, Palva S. Dynamic large-scale network synchronization from perception to action. Netw Neurosci. 2018;2:442–63.
107. Siebenhühner F, Wang SH, Arnulfo G, Lampinen A, Nobili L, Palva JM, et al. Genuine cross-frequency coupling networks in human resting-state electrophysiological recordings. PLoS Biol. 2020;18:e3000685.
108. Palva JM, Monto S, Kulashekhar S, Palva S. Neuronal synchrony reveals working memory networks and predicts individual memory capacity. Proc Natl Acad Sci USA. 2010;107:7580–5.
109. Palva S, Kulashekhar S, Hämäläinen M, Palva JM. Localization of cortical phase and amplitude dynamics during visual working memory encoding and retention. J Neurosci. 2011;31:5013–25.
110. Korhonen O, Palva S, Palva JM. Sparse weightings for collapsing inverse solutions to cortical parcellations optimize M/EEG source reconstruction accuracy. J Neurosci Methods. 2014;226:147–60.
111. Linkenkaer-Hansen K, Nikouline VV, Palva JM, Ilmoniemi RJ. Long-range temporal correlations and scaling behavior in human brain oscillations. J Neurosci. 2001;21:1370–7.
112. Zhigalov A, Arnulfo G, Nobili L, Palva S, Palva JM. Modular co-organization of functional connectivity and scale-free dynamics in the human brain. Netw Neurosci. 2017;1:143–65.
113. Zhigalov A, Arnulfo G, Nobili L, Palva S, Palva JM. Relationship of fast- and slow-timescale neuronal dynamics in human MEG and SEEG. J Neurosci. 2015;35:5385–96.
114. Puoliväli T, Palva S, Palva JM. Influence of multiple hypothesis testing on reproducibility in neuroimaging research: a simulation study and python-based software. J Neurosci Methods. 2020;337:108654.
115. Metin B, Roeyers H, Wiersema JR, van der Meere J, Sonuga-Barke E. A meta-analytic study of event rate effects on Go/No-Go performance in attention-deficit/hyperactivity disorder. Biol Psychiatry. 2012;72:990–6.
116. Münger M, Sele S, Candrian G, Kasper J, Abdel-Rehim H, Eich-Höchli D, et al. Longitudinal analysis of self-reported symptoms, behavioral measures, and event-related potential components of a cued Go/NoGo task in adults with attention-deficit/hyperactivity disorder and controls. Front Hum Neurosci. 2022;16:767789.
117. Liu Y, Hanna GL, Hanna BS, Rough HE, Arnold PD, Gehring WJ. Behavioral and electrophysiological correlates of performance monitoring and development in children and adolescents with attention-deficit/hyperactivity disorder. Brain Sci. 2020;10:79.
118. Aston-Jones G, Cohen JD. An integrative theory of locus coeruleus-norepinephrine function: adaptive gain and optimal performance. Annu Rev Neurosci. 2005;28:403–50.
119. Unsworth N, Robison MK. Working memory capacity and sustained attention: A cognitive-energetic perspective. J Exp Psychol Learn Mem Cogn. 2020;46:77–103.
120. Fisher JT, Hopp FR, Weber R. Cognitive and perceptual load have opposing effects on brain network efficiency and behavioral variability in ADHD. Netw Neurosci. 2023;7:1483–96.
121. Salmi J, Metwaly M, Tohka J, Alho K, Leppämäki S, Tani P, et al. ADHD desynchronizes brain activity during watching a distracted multi-talker conversation. Neuroimage. 2020;216:116352.
122. Corbetta M, Patel G, Shulman GL. The reorienting system of the human brain: from environment to theory of mind. Neuron. 2008;58:306–24.
123. Iemi L, Chaumon M, Crouzet SM, Busch NA. Spontaneous neural oscillations bias perception by modulating baseline excitability. J Neurosci. 2017;37:807–19.
124. D'Andrea A, Chella F, Marshall TR, Pizzella V, Romani GL, Jensen O, et al. Alpha and alpha-beta phase synchronization mediate the recruitment of the visuospatial attention network through the superior longitudinal fasciculus. Neuroimage. 2019;188:722–32.
125. Assem M, Hart MG, Coelho P, Romero-Garcia R, McDonald A, Woodberry E, et al. High gamma activity distinguishes frontal cognitive control regions from adjacent cortical networks. Cortex. 2023;159:286–98.
126. Minzenberg MJ, Firl AJ, Yoon JH, Gomes GC, Reinking C, Carter CS. Gamma oscillatory power is impaired during cognitive control independent of medication status in first-episode schizophrenia. Neuropsychopharmacology. 2010;35:2590–9.
127. Zhu Y, Liu L, Yang D, Ji H, Huang T, Xue L, et al. Cognitive control and emotional response in attention-deficit/ hyperactivity disorder comorbidity with disruptive, impulse-control, and conduct disorders. BMC Psychiatry. 2021;21:232.
128. Sidlauskaite J, Sonuga-Barke E, Roeyers H, Wiersema JR. Altered intrinsic organisation of brain networks implicated in attentional processes in adult attention-deficit/hyperactivity disorder: a resting-state study of attention, default mode and salience network connectivity. Eur Arch Psychiatry Clin Neurosci. 2016;266:349–57.
129. Luo X, Dang C, Guo J, Li D, Wang E, Zhu Y, et al. Overactivated contextual visual perception and response to a single dose of methylphenidate in children with ADHD. Eur Arch Psychiatry Clin Neurosci. 2024;274:35–44.
130. Sonuga-Barke E, Bitsakou P, Thompson M. Beyond the dual pathway model: evidence for the dissociation of timing, inhibitory, and delay-related impairments in attention-deficit/hyperactivity disorder. J Am Acad Child Adolesc Psychiatry. 2010;49:345–55.
131. Smit DJA, de Geus EJC, van de Nieuwenhuijzen ME, van Beijsterveldt CEM, van Baal GCM, Mansvelder HD, et al. Scale-free modulation of resting-state neuronal oscillations reflects prolonged brain maturation in humans. J Neurosci. 2011;31:13128–36.
132. Shaw P, Malek M, Watson B, Sharp W, Evans A, Greenstein D. Development of cortical surface area and gyrification in attention-deficit/hyperactivity disorder. Biol Psychiatry. 2012;72:191–7.
133. Shaw P, Ishii-Takahashi A, Park MT, Devenyi GA, Zibman C, Kasparek S, et al. A multicohort, longitudinal study of cerebellar development in attention deficit hyperactivity disorder. J Child Psychol Psychiatry. 2018;59:1114–23.
134. Smallwood J, Schooler JW. The science of mind wandering: empirically navigating the stream of consciousness. Annu Rev Psychol. 2015;66:487–518.
135. Forster S, Lavie N. High perceptual load makes everybody equal: eliminating individual differences in distractibility with load. Psychol Sci. 2007;18:377–81.
136. Lavie N, Hirst A, de Fockert JW, Viding E. Load theory of selective attention and cognitive control. J Exp Psychol Gen. 2004;133:339–54.
137. Michelini G, Palumbo IM, DeYoung CG, Latzman RD, Kotov R. Linking RDoC and HiTOP: A new interface for advancing psychiatric nosology and neuroscience. Clin Psychol Rev. 2021;86:102025.
138. Ibanez A, Kringelbach ML, Deco G. A synergetic turn in cognitive neuroscience of brain diseases. Trends Cogn Sci. 2024;28:319–38.
139. Deco G, Kringelbach ML. Great expectations: using whole-brain computational connectomics for understanding neuropsychiatric disorders. Neuron. 2014;84:892–905.

140. Ezaki T, Fonseca dos Reis E, Watanabe T, Sakaki M, Masuda N. Closer to critical resting-state neural dynamics in individuals with higher fluid intelligence. Commun Biol. 2020;3:1–9.
141. Schippers LM, Greven CU, Hoogman M. Associations between ADHD traits and self-reported strengths in the general population. Compr Psychiatry. 2024;130:152461 https://doi.org/10.1016/J.COMPPSYCH.2024.152461.
142. Geissler J, Romanos M, Hegerl U, Hensch T. Hyperactivity and sensation seeking as autoregulatory attempts to stabilize brain arousal in ADHD and mania?. Atten Defic Hyperact Disord. 2014;6:159–73.

ACKNOWLEDGEMENTS

We thank Anna Lampinen for assistance in collecting the neuropsychological data and Sami Karadeniz for assistance in collecting the MEG data. We also thank all subjects who participated in the study.

AUTHOR CONTRIBUTIONS

SP and JMP conceived the study and supervised the project. SP, JMP, JS, and IM were responsible for funding acquisition. BUC, JH, and HH were responsible for participant recruitment. HH, JH, JS, and IM performed experiments and managed the MEG and clinical data. HH and JH were responsible for data analysis and visualization. HH and SHW were responsible for data validation. HH, JH, and SP were responsible for writing the original draft of the manuscript. All authors were responsible for reviewing and editing the manuscript.

FUNDING

SP and JMP declare support for the research from the Sigrid Juselius Foundation. IM declares support for the research from the Ella and Georg Ehrnrooth Foundation. JS declares support for the research from the Academy of Finland (SA 1294761).

COMPETING INTERESTS

The authors declare no competing financial interests.

ADDITIONAL INFORMATION

Supplementary information The online version contains supplementary material available at https://doi.org/10.1038/s41398-026-04267-0.

Correspondence and requests for materials should be addressed to Satu Palva.

Reprints and permission information is available at http://www.nature.com/reprints

Publisher's note Springer Nature remains neutral with regard to jurisdictional claims in published maps and institutional affiliations.

Open Access This article is licensed under a Creative Commons Attribution 4.0 International License, which permits use, sharing, adaptation, distribution and reproduction in any medium or format, as long as you give appropriate credit to the original author(s) and the source, provide a link to the Creative Commons licence, and indicate if changes were made. The images or other third party material in this article are included in the article's Creative Commons licence, unless indicated otherwise in a credit line to the material. If material is not included in the article's Creative Commons licence and your intended use is not permitted by statutory regulation or exceeds the permitted use, you will need to obtain permission directly from the copyright holder. To view a copy of this licence, visit http://creativecommons.org/licenses/by/4.0/.

© The Author(s) 2026